Chemical Science

ROYAL SOCIETY OF CHEMISTRY

EDGE ARTICLE

View Article Online
View Journal | View Issue

Cite this: *Chem. Sci.*, 2022, **13**, 1706

All publication charges for this article have been paid for by the Royal Society of Chemistry

Received 6th December 2021
Accepted 17th December 2021

DOI: 10.1039/d1sc06803b

rsc.li/chemical-science

Why intermolecular nitric oxide (NO) transfer? Exploring the factors and mechanistic aspects of NO transfer reaction†

Sandip Das, [a] Kulbir, [a] Soumyadip Ray,[a] Tarali Devi,[b] Somnath Ghosh, [a] Sarvesh S. Harmalkar,[c] Sunder N. Dhuri,[c] Padmabati Mondal [a] and Pankaj Kumar *[a]

Small molecule activation and their transfer reactions in biological or catalytic reactions are greatly influenced by the metal-centers and the ligand frameworks. Here, we report the metal-directed nitric oxide (NO) transfer chemistry in low-spin mononuclear $\{Co(NO)\}^8$, $[(12\text{-TMC})Co^{III}(NO^{-})]^{2+}$ (**1-CoNO**, $S = 0$), and $\{Cr(NO)\}^5$, ($[(BPMEN)Cr(NO)(Cl)]^{+}$) (**4-CrNO**, $S = 1/2$) complexes. **1-CoNO** transfers its bound NO moiety to a high-spin $[(BPMEN)Cr^{II}(Cl_2)]$ (**2-Cr**, $S = 2$) and generates **4-CrNO** *via* an associative pathway; however, we did not observe the reverse reaction, *i.e.*, NO transfer from **4-CrNO** to low-spin $[(12\text{-TMC})Co^{II}]^{2+}$ (**3-Co**, $S = 1/2$). Spectral titration for NO transfer reaction between **1-CoNO** and **2-Cr** confirmed 1 : 1 reaction stoichiometry. The NO transfer rate was found to be independent of **2-Cr**, suggesting the presence of an intermediate species, which was further supported experimentally and theoretically. The experimental and theoretical observations support the formation of μ-NO bridged intermediate species ($\{Cr{-}NO{-}Co\}^{4+}$). Mechanistic investigations using ^{15}N-labeled-^{15}NO and tracking the ^{15}N-atom established that the NO moiety in **4-CrNO** is derived from **1-CoNO**. Further, to investigate the factors deciding the NO transfer reactivity, we explored the NO transfer reaction between another high-spin Cr^{II}-complex, $[(12\text{-TMC})Cr^{II}(Cl)]^{+}$ (**5-Cr**, $S = 2$), and **1-CoNO**, showing the generation of the low-spin $[(12\text{-TMC})Cr(NO)(Cl)]^{+}$ (**6-CrNO**, $S = 1/2$); however, again there was no opposite reaction, *i.e.*, from Cr-center to Co-center. The above results advocate clearly that the NO transfer from Co-center generates thermally stable and low-spin and inert $\{Cr(NO)\}^5$ complexes (**4-CrNO** & **6-CrNO**) from high-spin and labile Cr-complexes (**2-Cr** & **5-Cr**), suggesting a metal-directed NO transfer (cobalt to chromium, not chromium to cobalt). These results explicitly highlight that the NO transfer is strongly influenced by the labile/inert behavior of the metal-centers and/or thermal stability rather than the ligand architecture.

Introduction

In the biological system, the choice of metal-centers and the ligand frameworks significantly influence coordination chemistry, redox property, and various metalloenzymes' reactivity.[1] When it comes to small molecule activation, enzymatic and catalytic reactions, these properties become more prominent for selective biological reactions. For example, heme systems of particular proteins (NiRs) bind with nitric oxide (NO);[2] however, other proteins with similar heme groups do not show NO-activation,[3] and it is rare to have NO activation on different metal centers having the same coordination sphere.[4] Together, these parameters provide an excellent opportunity or challenge to the scientific community to study/explore the small molecules' interactions with metals in different ligand frameworks. Consequently, the transfer of coordinated ligands to another metal center has become the area of interest for the past few decades. Halide transfer reactions are one of the most explored reactions.[5] Some examples of intermolecular transfer of bound carbon monoxide (CO),[6] superoxide ($O_2^{\bullet-}$),[7] and peroxide (O_2^{2-})[8] were also reported. Nowadays, atom transfer reactions are an area of fundamental importance, particularly apparent in biological systems.[9] A number of metalloenzymes were reported to mediate the oxygen atom transfer (OAT) reactions,[10] specially molybdoenzymes such as nitrate reductase (NRs)[11] and C–H activation reactions.[12,13]

NO activation became an area of interest for chemists and biochemists due to the vast presence of metal-nitrosyls (M-NOs) in the biological system. Being a radical species, NO is widely

[a]*Department of Chemistry, Indian Institute of Science Education and Research (IISER), Tirupati 517507, India. E-mail: pankaj@iisertirupati.ac.in*

[b]*Humboldt-Universität zu Berlin, Institut für Chemie, Brook-Taylor-Straße 2, D-12489 Berlin, Germany*

[c]*School of Chemical Sciences, Goa University, Goa-403206, India*

† Electronic supplementary information (ESI) available. CCDC 2076723. For ESI and crystallographic data in CIF or other electronic format see DOI: 10.1039/d1sc06803b

known as a signal transduction molecule for its involvement in major biological processes, such as neurotransmission, vascular regulation, platelet disaggregation, and immune response to bacterial infections.[13] The deficiency of NO in the natural system hamper the processes described above and leads to several biological disorders, including atherothrombosis,[14] diabetic hypertension,[15] and chronic kidney disease.[16,17] In this regard, nitric oxide synthases (NOSs)[18] and nitrite reductases (NiRs)[2,19] accomplish the constant biosynthesis of NO. NOSs are a family of enzymes that catalyze the guanidine nitrogen oxidation in L-arginine to produce NO.[20] Whereas, in some mammalian and bacterial systems, NiRs catalyze the production of NO by NO_2^- reduction in the presence of protons, *i.e.*, $NO_2^- + e^- + 2H^+ \rightarrow NO + H_2O$.[21] In the biological system, NO acts as a double-edged sword, and overproduction can lead to the generation of several cytotoxic molecules.[22]

The coordination chemistry of M-NOs has a long history of understanding the fundamental aspects of binding, electronic arrangements, and reactivity.[23] Until now, several M-NOs have been synthesized and explored for different reactivities,[4b,24] including even a few reports on intermolecular NO transfer;[25] however, the mechanistic aspects of these reactions have rarely been explored. An extensive study of the NO transfer process may enlighten the NO transport process in the biological system. Earlier, Armor reported acid-promoted metal-dependent NO transfer from Co^{III} to Cr^{II} involving a labile aqua complex.[25e] Further studies suggest the transfer of the NO ligand at high acidic conditions due to axial NO ligand protonation.[26] Caulton and co-workers, in a study of NO transfer reactivity from Co to various metal complexes of Fe, Ru, Rh, and Co complexes, proposed that the NO transfers readily to the coordinatively unsaturated metal complexes, either *via* a simple NO transfer or *via* halide exchange pathway.[25c] Mu and Kadish speculated the effect of metal-center on a NO transfer reaction.[27] An intermediate species formation was also proposed before NO transfer, suggesting an association mechanism.[25a–e] Cook and co-workers, for the first time, reported a dissociative pathway in a NO transfer reaction from $Co(NO)(dmgH)_2$ to Hemoglobin (Hb).[28] Lippard and co-workers also testified a dissociated NO transfer pathway from Mn to Fe bearing a tropocarnado ligand.[25d] A μ-NO bridge intermediate was discussed in a NO transfer reaction of Ru to Fe-center of Hb and myoglobin (Mb); however, this has not been well identified or confirmed with experimental evidence.[25a] Recently, Nam and co-workers reported NO transfer reactivity influenced by ligand size and the spin-state of the acceptor/donor metal complexes.[29] These results suggest that the reaction mechanism and the intermediate involved in the intermolecular NO transfer reaction are inconsistent and depend on various factors; however, these reports lack a detailed mechanistic investigation. Here, the spectroscopic signatures for the proposed μ-NO bridge intermediate species need to be characterized in detail, which will surely help the scientific community understand the mechanistic insights of NO transfer reactions.

We herein report the NO transfer reactivity of a Co^{III}-nitrosyl complex, $[(12\text{-TMC})Co^{III}(NO^-)]^{2+}$ (**1-CoNO**),[4b,30] bearing a 12-TMC ligand (12-TMC = 1,4,7,10-tetramethyl-1,4,7,10-tetraazacyclododecane) with a Cr^{II}-complex, $[(BPMEN)Cr^{II}(Cl)_2]$ (**2-Cr**), bearing BPMEN ligand (BPMEN = *N*,*N*′-bis(2-pyridylmethyl)-1,2-diaminoethane), and this reaction generates $[(12\text{-TMC})Co^{II}]^{2+}$ (**3-Co**) and $[(BPMEN)Cr(Cl)(NO)]^+$ (**4-CrNO**) (Scheme 1, reaction II). Mechanistic insight into the reaction suggests that the reaction goes through an associative pathway and is also supported by determining various physical parameters (Scheme 2, reaction I & II). We have observed the generation of an intermediate, proposed to be μ-NO bridge intermediate species ($\{Cr–NO–Co\}^{4+}$), formation prior to the intermolecular NO transfer and well-characterized spectroscopically for the first time. The ligand framework plays a critical role in the NO transfer chemistry;[25f] however, we can not ignore the metal-centers' properties in M-NOs, *i.e.*, spin-states and labile/inert behavior, and also the M-NOs thermal stability. To understand the factors deciding the NO transfer chemistry, we performed NO transfer reactivity from **1-CoNO** to $[(12\text{-TMC})Cr^{II}(Cl)]^+$ (**5-Cr**), which generates ($[(12\text{-TMC})Cr(NO)(Cl)]^+$) (**6-CrNO**) (Scheme 3), and *vice versa* (**6-CrNO** to **3-Co**; no NO transfer). This chemistry established the labile-inert behavior of metal-centers through a significant impact in the NO transfer reactions rather than the influence of the ligand framework.

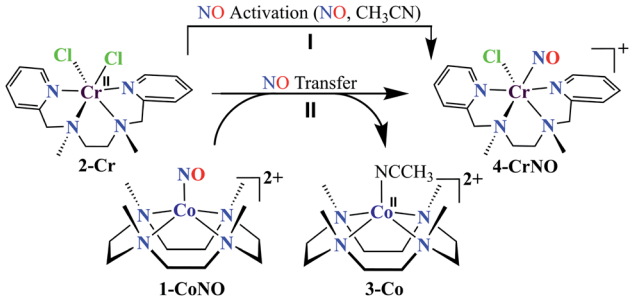

Scheme 1

Results

Synthesis of Cr-nitrosyl complex [(BPMEN)Cr(NO)(Cl)]Cl (4-CrNO)

The initial Cr^{II}-complex $[(BPMEN)Cr^{II}(Cl)_2]$ was synthesized by adding BPMEN ligand to a stirring solution of $CrCl_2$ (ESI,† Experimental Section (ES)). The addition of excess $NO_{(g)}$ (Fig. S1 in the ESI† shows a schematic diagram of the $NO_{(g)}$ purification and handling process) to the CH_3CN solution of **2-Cr** at RT under an Ar atmosphere resulted in the generation of **4-CrNO** (λ_{max} = 600, ε = 110 M^{-1} cm^{-1}, red line) within 5 min and isolated as a solid product (Fig. 1a and S2a, ESI,† ES) (Scheme 1, reaction I). Electrospray ionization mass spectrometry (ESI-MS) of **4-CrNO** showed a prominent ion peak at *m*/*z* 387.1, whose mass and isotope distribution patterns correspond to $[(BPMEN)Cr(NO)(Cl)]^+$ (calcd *m*/*z* 387.1) (Fig. 1b). When the reaction was carried out with ^{15}N-labeled NO (^{15}NO), the mass peak corresponding to $[Cr(BPMEN)(^{15}NO)(Cl)]^+$ appears at *m*/*z* 388.1 (calcd *m*/*z* 388.1) (inset, Fig. 1b and S2b; ESI†). This one unit shift in mass value upon substitution of NO by ^{15}NO indicates that **4-**

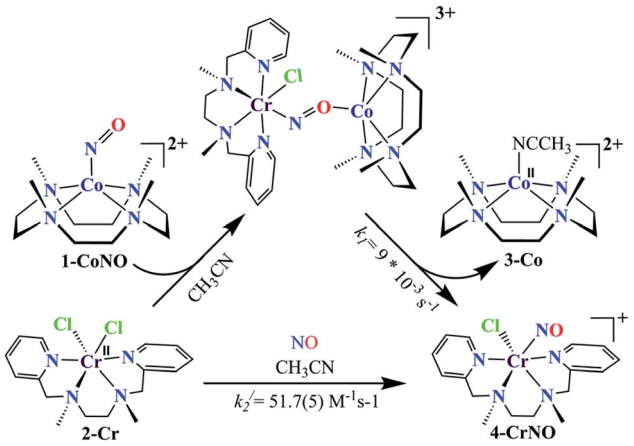

Scheme 2

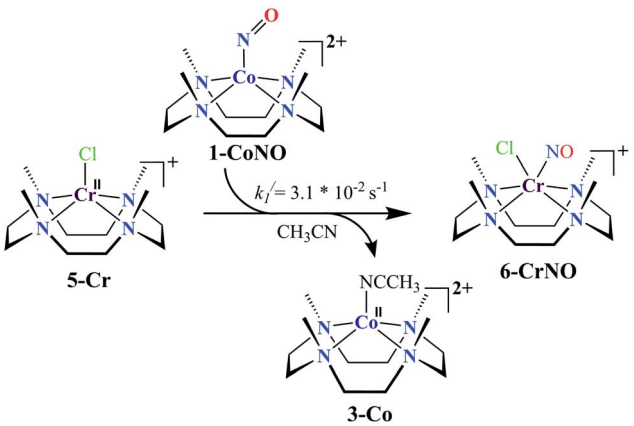

Scheme 3

CrNO contains an NO moiety attached to the Cr-center. The FT-IR spectrum is also consistent with the exact formulation of **4-CrNO**, revealing a linear NO with a typical M-NO stretching at 1690 cm^{-1}, which shifted to 1650 cm^{-1} when **4-CrNO** was prepared using ^{15}NO (inset, Fig. 1a, S2c and S2d; ESI†).[31] The ^{1}H NMR of **4-CrNO** does not exhibit any signal for aromatic protons, suggesting a paramagnetic Cr-center (ESI,† Fig. S3a). Further, the magnetic moment calculated by Evans' method revealed a magnetic moment of 1.68, which corresponds to a low-spin Cr-centre (d^5, $S = 1/2$) in complex **4-CrNO** (ESI,† Fig. S3b), which can be assigned as $\{Cr(NO)\}^5$.[32] Further, **4-CrNO** was structurally characterized *via* single-crystal X-ray crystallography. The NO ligand is coordinated to a Cr-center in an end-on fashion with a distorted octahedral geometry. The Cr(1)–N(5)–O(1) bond angle of **4-CrNO** was found to be 174.0(11)° suggesting sp hybridization of N-atom, as explained in other reports.[31a] Hence, NO coordination to the low-spin Cr-center was confirmed, which was further consistent with our assignment of this complex as $\{Cr(NO)\}^5$ species (Fig. 2, S4, Tables S1 and S2; ESI,† ES).[33]

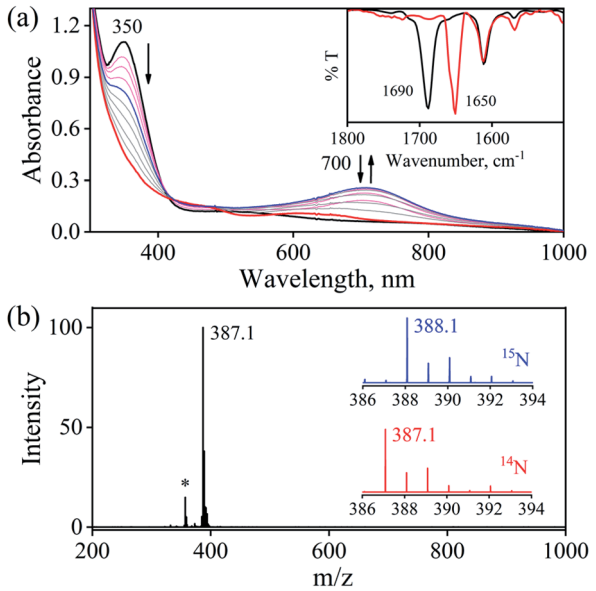

Fig. 1 (a) UV-Visible spectral changes of **2-Cr** (1 mM, black line) upon addition of $NO_{(g)}$ in CH_3CN under Ar at 298 K. Inset: FT-IR spectra of **4-CrNO** (black line) and **4-Cr^{15}NO** (red line) in KBr. (b) ESI-MS spectra of **4-CrNO** The peak at *m/z* 387.1 is assigned to $[(BPMEN)Cr(NO)(Cl)]^+$ (calcd *m/z* 387.1). Inset: isotopic distribution pattern for **4-CrNO** (red line) and **4-Cr^{15}NO** (blue line). The peak at *m/z* 357.1 marked with asterisk is assigned to $[(BPMEN)Cr(Cl)]^+$, which is the starting Cr^{II}-complex.

NO transfer reaction from 1-CoNO to 2-Cr

To further understand the NO-coordination chemistry, we explored NO transfer reactions between cobalt (**1-CoNO**) and chromium complexes (**2-Cr** & **5-Cr**), having different or alike ligand frameworks to determine the fundamental parameters behind NO transfer chemistry. When CH_3CN solution of **4-CrNO** reacted with an equivalent amount of **3-Co** under Ar atmosphere, we did not observe any significant change in the UV-Visible spectra except a new band at 485 nm, corresponding to **3-Co** (ESI,† Fig. S5). In contrast to the NO transfer from complex **4-CrNO** to **3-Co**, the reverse reaction, *i.e.*, NO transfer from **1-CoNO** to **2-Cr**, showed a visible color change from pink to bluish-green. The addition of one equivalent of **2-Cr** to **1-**

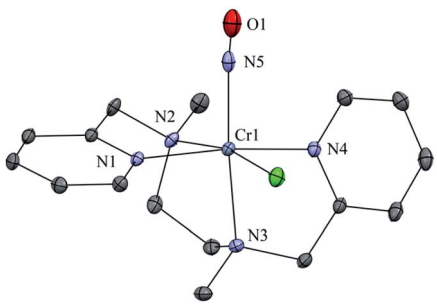

Fig. 2 Displacement ellipsoid plot (20% probability) of **4-CrNO** at 296 K. Disorder in N-atom of NO ligand is refined, anion and H-atoms have been removed for clarity.

CoNO immediately showed the generation of a new band (λ_{max} = 700 nm, blue line) (Fig. 3a), proposed to be an intermediate, which then slowly changed to a new absorption band (λ_{max} = 600 nm, red line), which corresponds to the absorption spectrum of **4-CrNO** (Fig. 3b and S6a; ESI†) (Scheme 2, reaction I & II). The final UV-Visible spectrum of the above NO transfer reaction was confirmed as the sum of complexes **3-Co** and **4-CrNO**, further supporting the NO transfer from Co to Cr-center (ESI,† Fig. S6b). The NO transfer reaction was established by the spectroscopic titration at 370 nm for the decomposition of **1-CoNO**, demonstrating that the ratio-metric equivalent of complex **2-Cr** to **1-CoNO** was 1 : 1 (Fig. 4). We further characterized the generation of this intermediate by FT-IR spectroscopy to follow the reaction mechanism. The addition of **2-Cr** to the solution of **1-CoNO** showed a new peak at 1520 cm^{-1}, which shifted to 1491 cm^{-1} when the reaction was performed with **1-Co^{15}NO** (Inset, Fig. 3a), suggesting the generation of μ-NO bridged species[34] {BPMEN-Cr–NO–Co-12-TMC}$^{4+}$ ({Cr–NO–Co}$^{4+}$), in the NO transfer reaction from Co to Cr-center. Additionally, EPR measurements were performed to trap the intermediate. In the low-temperature EPR measurements, we observed the formation of an intermediate species (g = 2.03) that shifted to a signal (g = 1.99) (inset, Fig. 3b) characteristic to the EPR signal of **4-CrNO**. This EPR spectrum suggests that the NO moiety is more on the Cr-center than Co-center in the {Cr–NO–Co}$^{4+}$ intermediate species, as both **1-CoNO** and **2-Cr** are EPR silent and only **4-CrNO** showed a peak in this range of g-values. Then, we further tried to characterize the intermediate *via* ESI-MS. However, being a thermally unstable moiety, the intermediate species decomposes under the mass spectrometry instrumental environment even at low temperatures and gives a peak for **4-CrNO** and **3-Co**, and efforts to characterize the intermediate become futile.

Furthermore, intermolecular NO transfer was confirmed by various spectroscopic techniques. The FT-IR spectrum of the reaction mixture obtained after the completion of the reaction of **2-Cr** with **1-CoNO**, in the KBr palette, exhibited a peak at 1690 cm^{-1}, which shifted to 1650 cm^{-1} when the reaction was carried out using ^{15}N labelled-NO complex **1-CoNO** (**1-Co^{15}NO**) (ESI,† Fig. S7a). The aforesaid FT-IR spectrum superimposes the FT-IR spectrum of an independently prepared equimolar mixture of **3-Co** and **4-CrNO**, again confirming the generation of {Cr(NO)}^{5} (ESI,† Fig. S7b). The ESI-MS of the above reaction mixture showed prominent ion peaks at m/z 143.6, 322.1, and 387.1, respectively, and their mass and isotope distribution patterns correspond to [(12-TMC)Co]$^{2+}$ (calcd m/z 143.6), [(12-TMC)Co(Cl)]$^+$ (calcd m/z 322.1), and [(BPMEN)Cr(Cl)(NO)]$^+$ (calcd m/z 387.1) (Fig. 3c). When the above reaction was performed by using **1-Co^{15}NO**, the mass peak shifted by one unit

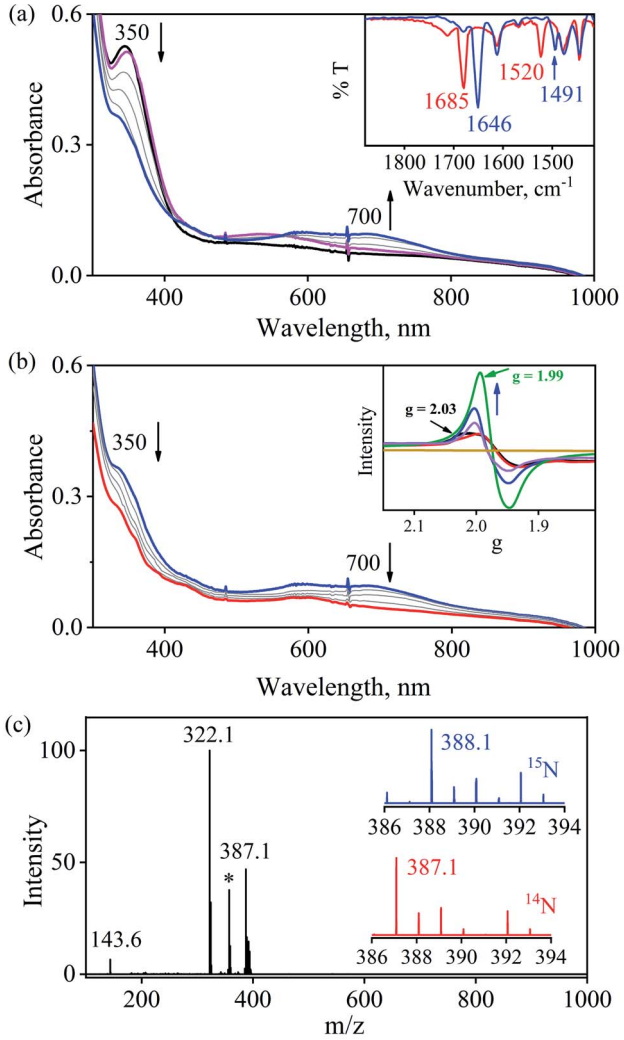

Fig. 3 (a) UV-Visible spectral changes showing the formation of an intermediate species (blue line) in the reaction of **2-Cr** (0.50 mM, black line) with **1-CoNO** (0.50 mM) under an Ar atmosphere in CH_3CN at 273 K. Inset: FT-IR spectra of the reaction solution of **1-CoNO** with **2-Cr** (red line) and **1-Co^{15}NO** with **2-Cr** (blue line). (b) Decomposition of the intermediate species to **4-CrNO** (red line). Inset: time-dependent EPR spectra of intermediate formation (black line) in the reaction of **2-Cr** and **1-CoNO** and finally conversion to end product (**4-CrNO**, green line) in CH_3CN at 77 K (c) ESI-MS spectra of the reaction mixture obtained in the reaction of **1-CoNO** with **2-Cr**. The peaks at m/z 387.1, 322.1, 143.6 are assigned to [(BPMEN)Cr(NO)(Cl)]$^+$ (calcd m/z 387.1), [(12-TMC)Co(Cl)]$^+$ (calcd m/z 322.1) and [(12-TMC)Co]$^{2+}$ (calcd m/z 143.6). The peak at m/z 357.1 marked with an asterisk is assigned to [(BPMEN)Cr(Cl)]$^+$. Isotopic distribution pattern for **4-CrNO** (red line) and **4-Cr^{15}NO** (blue line).

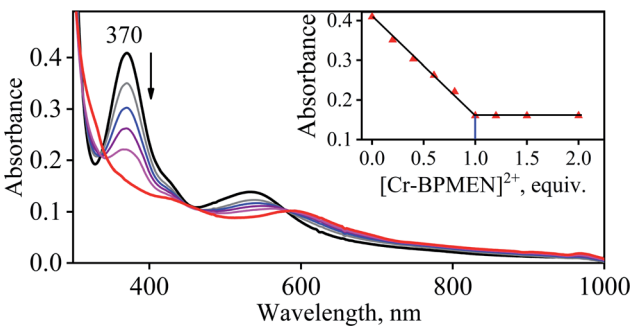

Fig. 4 UV-Vis spectral changes observed in the reaction **1-CoNO** with **2-Cr** (in the increments of 0, 0.20, 0.40, 0.60, 0.80, 1.0, 1.2, 1.5, 2.0 equivalent) in CH_3CN under Ar at 298 K.

and exhibited a prominent peak at *m/z* 388.1, which corresponds to $[(BPMEN)Cr(Cl)(^{15}NO)]^+$ and confirms the transfer of Co-bound NO to Cr-center (Fig. 3c and S7c, ESI†). The ^{1}H-NMR of the reaction mixture does not show any signals for the protons of the 12-TMC ring, which was initially present for **1-CoNO** (d^6, $S = 0$), suggesting the generation of **3-Co** (low spin d^7, $S = 1/2$) (ESI,† Fig. S8).[4b,25f] Further, ^{1}H-NMR titration also confirmed the 1 : 1 stoichiometry of **2-Cr** to **1-CoNO** (ESI,† Fig. S9). Based on the above evidence, we can conclude that complexes **3-Co** and **4-CrNO** were generated in the reaction of **1-CoNO** with **2-Cr**.

DFT calculations and experimental details for mechanistic insight into the NO transfer reaction of 1-CoNO with 2-Cr

From the spectroscopic and kinetic results, it is evident that the reaction is going through the formation of a bridged NO intermediate species. However, due to the instability of this intermediate, we were unable to characterize it structurally. Therefore, we investigated the reaction pathway of the intermediate formation by carrying out a DFT calculation. DFT calculation suggests the formation of an isonitrosyl-Co complex in the first transition state (TS_1) with an energy barrier of 14.66 kcal mol^{-1} (Fig. 5). In the next step, NO binds to the Cr *via* the N-donor site, which is −2.25 kcal mol^{-1} lower in energy than the reactant and therefore formed a thermodynamically favored side-on bound $\{Cr–NO–Co\}^{4+}$ intermediate species.[35] The experimental results well justified this; the influence of both the metal-centers leads to the lower stretching frequency from 1703 cm^{-1} for **1-CoNO** to 1520 cm^{-1} for the side on bonded $\{Cr–NO–Co\}^{4+}$ species. In addition to IR spectroscopy, a parallel trend was observed in low-temperature EPR measurements. When we reacted **1-CoNO** with **2-Cr**, a new peak

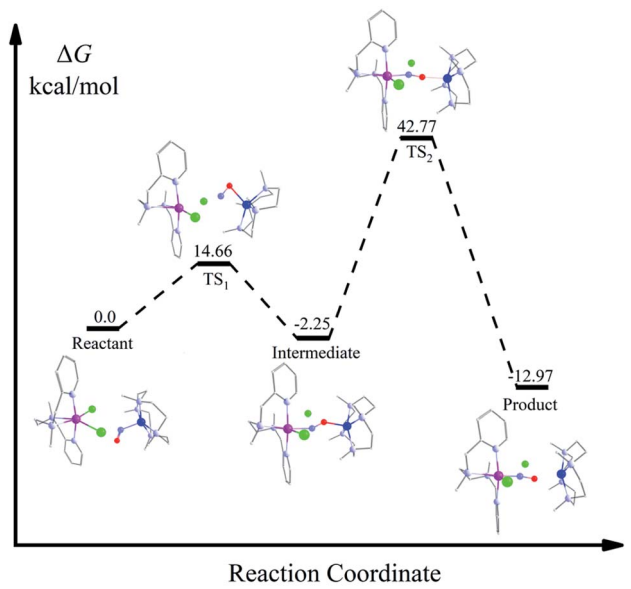

Fig. 5 : DFT-calculated associative reaction profile of NO-transfer from **1-CoNO** to **2-Cr** initiated from a μ-NO-bridged intermediate $\{Cr–NO–Co\}^{4+}$.

formation for the intermediate species was observed with $g = 2.03$, corresponding to a low spin Cr-center having a strong interaction of the N-atom of NO moiety to the Cr-center than Co-center (distance of N-atom of NO in intermediate, Cr–N = 228 pm and Co–N = 303 pm). This peak shifted to $g = 1.99$ (inset: Fig. 3b), corresponding to **4-CrNO** when the NO transfer completes. Further, the coordinated NO moiety undergoes dissociation leading to the final NO transfer product. The highest lying transition state TS_2 along the reaction profile is 42.77 kcal mol^{-1}, more elevated than the reactant, significantly higher than the 14.66 kcal mol^{-1} barrier of TS_1, indicating that the dissociation of the intermediate to the product is the rate-determining step. This high-energy TS_2 leads the reaction to a first-order reaction independent of the concentration of both **1-CoNO** and **2-Cr**.

NO transfer reaction from 1-CoNO to 5-Cr

Complex **1-CoNO** eventually showed the NO transfer reactivity with $[(12\text{-TMC})Cr(Cl)]^+$ (**5-Cr**) (Scheme 3). The addition of one equivalent of **5-Cr** to the solution of **1-CoNO** leads to the disappearance of the band at 370 nm (Fig. 6a). Further analysis of the reaction mixture by the ESI-MS measurements showed prominent ion peaks at *m/z* 143.6, 345.1 and 322.1, corresponding to $[(12\text{-TMC})Co]^{2+}$ (calcd *m/z* 143.6), [(12-TMC)

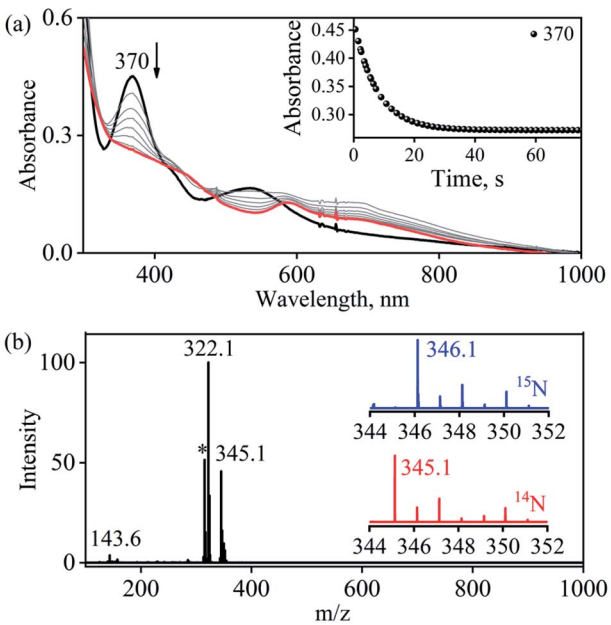

Fig. 6 (a) UV-Visible spectral changes obtained in the NO transfer from **1-CoNO** (0.50 mM; black line) to **5-Cr** (0.50 mM) to form **6-CrNO** (brick red line) under an Ar atmosphere in CH_3CN at 273 K. Inset: time course of the decomposition of **1-CoNO** monitored at 370 nm (black circles) (b) ESI-MS spectra of the reaction mixture obtained in the reaction of **5-Cr** with **1-CoNO**. The peaks at *m/z* 345.1, 322.1, 143.6 are assigned to $[(12\text{-TMC})Cr(NO)(Cl)]^+$ (calcd *m/z* 345.1) $[(12\text{-TMC})Co(Cl)]^+$ (calcd *m/z* 322.1) and $[(12\text{-TMC})Co]^{2+}$ (calcd *m/z* 143.6). The peak at *m/z* 314.1 marked with asterisk is assigned to $[(12\text{-TMC})Cr^{II}(Cl)]^+$ (calcd *m/z* 314.1). Inset: isotopic distribution pattern for **6-CrNO** (red line) and **6-Cr^{15}NO** (blue line).

$Cr(NO)(Cl)]^+$ (**6-CrNO**) (calcd *m*/*z* 345.1), and $[(12\text{-TMC})Co(Cl)]^+$ (calcd *m*/*z* 322.1), respectively (Fig. 6b). The mass peaks shifted by one unit to *m*/*z* 346.1 corresponds to $[(12\text{-TMC})Cr(^{15}NO)(Cl)]^+$ (calcd *m*/*z* 346.1) when the reaction is performed with **1-Co^{15}NO** confirms the NO transfer from complex **1-CoNO** to **5-Cr** (ESI,† Fig. S12). Further, stoichiometric titration for NO transfer reaction was followed at 370 nm for the decomposition of **1-CoNO**, which showed that the ratio-metric equivalent of complex **5-Cr** to **1-CoNO** was 1 : 1 (ESI,† Fig. S13).

Discussion

The mechanistic insights of the NO transfer reaction

To elaborate on the chemistry involved in the NO transfer reaction of **1-CoNO** with **2-Cr**, why is it happening? We then explored the NO transfer reaction's mechanistic insight. There are two possible mechanistic approaches for the NO transfer reactions in M-NOs, *i.e.*, associative or dissociative pathways (*vide infra*).[25a,25d,25f] As shown in Fig. 3, the reaction of **1-CoNO** with **2-Cr** is proceeding *via* the formation of an intermediate species (Fig. 3a, blue line) before generating the final product (Fig. 3b, red line), suggesting an associative mechanistic pathway. The UV-Visible spectrum of this intermediate species is different from the sum of the spectra of complexes **1-CoNO** + **2-Cr**, indicating that it is a new species rather than the mixture of **1-CoNO** & **2-Cr** (ESI,† Fig. S10). Suppose NO transfer is going through an associative pathway, then the dissociation of the intermediate species should be the rate-determining step. In that case, the reaction rate will be independent of **2-Cr**.[25f] Kinetics study revealed that the reaction rate was independent of the concentration of **2-Cr**, suggesting an associative intermediate species before NO transfer. In addition, the DFT calculation suggests an energy barrier of 42.77 kcal mol^{-1} in TS_2, a 28 kcal mole^{-1} higher-lying transition state than TS_1. Due to this higher energy barrier, the formation of the product from intermediate *via* TS_2 becomes slow and makes the reaction first order. Further, the formation of a peak at 1520 cm^{-1} in IR spectroscopy also supports the generation of a μ-NO bridged[34] transient species (Scheme 2) in the above reaction.[25b,25d,36]

The NO transfer reaction between **1-CoNO** and **2-Cr** was found to be following the first-order kinetic with a first-order rate constant (k_1) of 9×10^{-3} s^{-1}. Hence, the dissociation of the proposed $\{Cr\text{–}NO\text{–}Co\}^{4+}$ intermediate is supposed to be a rate-determining step, which is $\sim 10^3$ times slower than the earlier reported second-order formation rate-constant of **1-CoNO** ($k_2 = 12(1)$ M^{-1} s^{-1}).[4b] To find the driving forces of the NO transfer reaction, the second-order rate constant (k_2') and equilibrium constant (K_{eq}') of the formation of **4-CrNO** were determined and found to be 51.7(5) M^{-1} s^{-1} and 2.27×10^3 M^{-1} (ESI,† Fig. S11), respectively, which are ∼4 times and ∼2.5 times larger than the k_2 (12(1) M^{-1} s^{-1}) and K_{eq} (8.90×10^2 M^{-1}) of **1-CoNO**, respectively. This comparison of the rate-constants and equilibrium constants suggests clearly that the dissociation of the $\{Cr\text{–}NO\text{–}Co\}^{4+}$ intermediate should generate thermodynamically more stable molecules **4-CrNO** & **3-Co**, as proposed by the second-order rate constant and equilibrium constant for **1-CoNO** & **4-CrNO**.

Table 1 Activation Parameters for 1-CoNO, 4-CrNO and 6-CrNO

Complex	$\Delta H^{\ddagger}$ (kcal mol^{-1})	$\Delta S^{\ddagger}$ (cal mol^{-1} K)	$\Delta G^{\ddagger}_{298\ K}$ (kcal mol^{-1})
1-CoNO	3.93 ± 0.2	−41.94 ± 0.6	16.43 ± 0.2
4-CrNO	7.32 ± 0.3	−28.15 ± 1.4	15.71 ± 0.3
6-CrNO	5.21 ± 0.06	−36.77 ± 0.3	16.17 ± 0.12

Further, various thermodynamic properties were also determined for the generation of **1-CoNO** & **4-CrNO** (Table 1), which suggests that the formation of **4-CrNO** ($\Delta G^{\ddagger} = 15.71$ kcal mol^{-1}, $\Delta G^0 = -4.57$ kcal mol^{-1}) is thermodynamically more favorable than the formation of **1-CoNO** ($\Delta G^{\ddagger} = 16.43$ kcal mol^{-1}, $\Delta G^0 = -4.02$ kcal mol^{-1}). The thermodynamic stability of these molecules can also be explained based on the labile and inert behavior of the metal-centers.[37] The generation of an inert species **4-CrNO** (low spin d^5, $S = 1/2$) from a highly labile **2-Cr** (high spin d^4, $S = 2$) is one of the major driving forces of NO transfer, as reported in many other reports.[25f,37] In addition to labile and inert parameters and second-order formation rate constants for **1-CoNO** & **4-CrNO**, thermodynamic parameters (Table 1) further support our hypothesis as the generation of **3-Co** & **4-CrNO** from **1-CoNO** & **2-Cr** is due to the lower free energy for **4-CrNO** than **1-CoNO**, making the NO transfer reaction more spontaneous. Thus, apart from the various parameters (*vide supra*), other factors may affect the NO transfer reactivity. Logically thinking about the NO transfer chemistry clarifies that this reaction depends not only on various metal-center parameters,[25d] but also on the ligand frameworks, which may influence the transfer of NO from Co to Cr metal-center.[25f]

With an aim to determine the effect of the ligand frameworks, the NO transfer reaction was performed between Co and Cr bearing the same 12-TMC ligand framework. Complex **1-CoNO** also showed NO transfer to **5-Cr** and generated **6-CrNO**. While further exploring the reaction mechanism, we have investigated the reaction of **5-Cr** with **1-CoNO** in various ratios. The characteristic UV-Visible peaks of **1-CoNO** overlap with **5-Cr** made it difficult to perform the kinetic comparison in the presence of the higher amounts of **5-Cr**. Complex **1-CoNO** is thermodynamically stable and does not show any natural decay (ESI,† Fig. S14); hence, the NO transfer's plausible mechanism from **1-CoNO** to **5-Cr** suggests that the reaction may go through a transient intermediate species. We did not observe any intermediate species formation in the UV-Visible or FT-IR spectral measurements (Fig. 6a), which suggests that the strain between the 12-TMC ligand frameworks of **1-CoNO** & **5-Cr** causes a fast transfer of NO from Co to Cr-center. Since the NO transfer is first-order in nature, the formation of **6-CrNO** is believed to be the rate-determining step, which is equal to the overall reaction rate with a rate constant (k_1') of 3.1×10^{-2} s^{-1}. The second-order rate constant (k_2'') and equilibrium constant (K_{eq}'') of the formation of **6-CrNO** were also determined and found to be 29.3(2) M^{-1} s^{-1} and 1.48×10^3 M^{-1}, respectively, which are ∼2.5 times and ∼1.6 times larger than the second-order rate constant and equilibrium constant of **1-CoNO**,[25f] hence explaining why NO transfers from Co to Cr-center. In

addition, other thermodynamic parameters for **1-CoNO** ($\Delta G^{\ddagger}$ = 16.43 kcal mol^{-1}, $\Delta G^{0} = -4.02$ kcal mol^{-1}) and **6-CrNO** ($\Delta G^{\ddagger}$ = 16.17 kcal mol^{-1}, $\Delta G^{0} = -4.32$ kcal mol^{-1}) further supports why NO transfer reaction between **1-CoNO** & **5-Cr** generates **6-CrNO** (Table 1). In addition to the above experimental results and their interpretations, labile and inert nature of more stable **6-CrNO** (low spin d^5, $S = 1/2$, inert) (Fig. S15a†) and less stable **5-Cr** (high spin d^4, $S = 2$, labile) (Fig. S15b†) suggests a huge change in the spin state, which promotes the reaction to move in the forward direction.[37,38] The above discussion suggests that the ligand frameworks may influence the intermediate's stability and the rate of NO transfer; however, when it comes to the net transfer of coordinated NO moiety from one metal to another, it largely depends upon the stability of the metal-center and various other physical parameters.

Conclusion

In this report, for the very first time, we have demonstrated the NO transfer reactivity of Co^{III}-nitrosyl, which can be regulated by (a) the thermal stability of the end products, (b) by varying the ligand frameworks (open chain/cyclic) of the supporting ligands, and (c) the change in the labile/inert nature of Cr metal-center before and after NO coordination. Here, we explored the NO transfer reaction of $[(12\text{-TMC})Co(NO)]^{2+}$ (**1-CoNO**) with a Cr^{II}-complex, $[(BPMEN)Cr^{II}(Cl)_2]$ (**2-Cr**). For the very first time, we spectroscopically characterized (by UV-Visible, FT-IR, and EPR) the formation of a μ-NO bridged intermediate $\{BPMEN\text{-}Cr\text{–}NO\text{–}Co\text{-}12\text{-}TMC\}^{4+}$ ($\{Cr\text{–}NO\text{–}Co\}^{4+}$) before the NO transfer from **1-CoNO** to **2-Cr**, generating $[(BPMEN)Cr(NO)(Cl)]^{+}$ (**4-CrNO**) (Scheme 2), with no NO transfer of Cr-bound NO. These results were interpreted based on the significant thermal stability of $\{CrNO\}^5$, explained based on various physical parameters, *i.e.*, rate constant (k), Gibbs free energy of activation (ΔG), and labile-inert nature of metal-centers. The second-order rate constant (k_2') and equilibrium constant (K_{eq}') of the formation of **4-CrNO** was ~4 times and ~2.5 times that of **1-CoNO**; subsequently, it pushes the NO transfer from Co to Cr-center to generate **4-CrNO**. The free energy of activation of **4-CrNO** is lower than that of **1-CoNO**; hence, driving the NO transfer reaction towards the forward direction to generate thermodynamically more inert/stable **4-CrNO**. Also, the formation of an inert **4-CrNO** (low spin d^5, $S = 1/2$) from a labile **2-Cr** (high spin d^4, $S = 2$) is another major driving force of NO transfer to achieve more stability.[25f,37] Additionally, the structure of the intermediate was predicted from a DFT calculation. The results from DFT calculations suggest a μ-NO bridged intermediate that binds in a side-on fashion to both Co and Cr-center, having a strong interaction of NO with Cr-center than Co-center, and is in qualitative agreement with other experimental results. NO transfer reaction was also analyzed by taking $[(12\text{-TMC})Cr^{II}(Cl)]^{+}$ (**5-Cr**) to evaluate the effect of the ligand framework. Complex **1-CoNO** showed the transfer of its NO moiety to **5-Cr** without observing any intermediate species generating thermodynamically stable **6-CrNO** (*vide supra*), which may be due to the high strain caused by the methyl groups in the 12-TMC ligand and its cyclic nature.[25f] The BPMEN is an open-chain ligand with only two methyl groups, probably making it adapt/change its geometry to form the proposed intermediate. This is quite interesting because two Cr^{II}-complexes show NO transfer reactivity due to the higher stability of the final $\{CrNO\}^5$ adduct; however, the ligand frameworks significantly influence the stability of the intermediate and hence control the reaction's fate. The present results describe original findings, where the generation of μ-NO bridged intermediate was observed before NO transfer and characterized spectroscopically and theoretically.

Data availability

All the required data already provided in the ESI† and manuscript.

Author contributions

PK & SD discovered/conceptualized the initial project. SD, Kulbir, & SG carried out the different experiments and gathered the data. SR & PM carried out the DFT calculation, and PM analyzed the data. PK & TD interpreted the experimental results. PK & SD wrote the first draft of the article. PK, TD & PM corrected the manuscript, finalized the final draft, and guided during the revision. PK followed and guided the whole project work.

Conflicts of interest

There are no conflicts to declare.

Acknowledgements

This work was supported by Grants-in-Aid (Grant No. EEQ/2016/000466) from SERB-DST and DAAD (ID: 57552334). S. D., Kulbir, S. G., S. R. thank IISER Tirupati for their fellowship. PM thanks DST, SERB, GoI (SRG/2020/001354) for financial support. We thank Mr Vamsi Katta (IISER Tirupati) and Mr S. Subramanian (SAIF, IIT Madras) for doing some specific experiments. Thanks to SAIF (IIT Madras) for the EPR facility.

References

1 (*a*) L. R. MacGillivray and C. M. Lukehart, *Metal–organic framework materials*, John Wiley & Sons, 2014; (*b*) H. J. Kruger, G. Peng and R. H. Holm, *Inorg. Chem.*, 2002, **30**, 734–742; (*c*) X. J. Yao, G. Velez Ruiz, M. R. Whorton, S. G. Rasmussen, B. T. DeVree, X. Deupi, R. K. Sunahara and B. Kobilka, *Proc. Natl. Acad. Sci. U. S. A.*, 2009, **106**, 9501–9506; (*d*) K. Oettl and R. E. Stauber, *Br. J. Pharmacol.*, 2007, **151**, 580–590; (*e*) J. Anastassopoulou, *J. Mol. Struct.*, 2003, **651–653**, 19–26.

2 E. I. Tocheva, F. I. Rosell, A. G. Mauk and M. E. Murphy, *Science*, 2004, **304**, 867–870.

3 (*a*) J. B. Weinberg, Y. Chen, N. Jiang, B. E. Beasley, J. C. Salerno and D. K. Ghosh, *Free Radicals Biol. Med.*, 2009, **46**, 1626–1632; (*b*) R. A. Firth, H. A. O. Hill,

J. M. Pratt, R. G. Thorp and R. J. P. Williams, *J. Chem. Soc. A*, 1969, 381–386, DOI: 10.1039/j19690000381.

4 (*a*) A. Yokoyama, K. B. Cho, K. D. Karlin and W. Nam, *J. Am. Chem. Soc.*, 2013, **135**, 14900–14903; (*b*) P. Kumar, Y. M. Lee, Y. J. Park, M. A. Siegler, K. D. Karlin and W. Nam, *J. Am. Chem. Soc.*, 2015, **137**, 4284–4287.

5 (*a*) T. J. Meyer and H. Taube, in *Comprehensive Coordination Chemistry*, Pergamon Press, Oxford, ed Wilkinson G., 1987, p. 331; (*b*) T. M. Shea, S. P. Deraniyagala, D. B. Studebaker and T. D. Westmoreland, *Inorg. Chem.*, 1996, **35**, 7699–7703.

6 T. Morimoto, K. Fuji, K. Tsutsumi and K. Kakiuchi, *J. Am. Chem. Soc.*, 2002, **124**, 3806–3807.

7 S. Hong, K. D. Sutherlin, J. Park, E. Kwon, M. A. Siegler, E. I. Solomon and W. Nam, *Nat. Commun.*, 2014, **5**, 5440.

8 (*a*) J. Cho, R. Sarangi, H. Y. Kang, J. Y. Lee, M. Kubo, T. Ogura, E. I. Solomon and W. Nam, *J. Am. Chem. Soc.*, 2010, **132**, 16977–16986; (*b*) J. Cho, R. Sarangi, J. Annaraj, S. Y. Kim, M. Kubo, T. Ogura, E. I. Solomon and W. Nam, *Nat. Chem.*, 2009, **1**, 568–572.

9 L. K. Woo, *Chem. Rev.*, 2002, **93**, 1125–1136.

10 (*a*) P. R. O. De Montellano, *Cytochrome P450: structure, mechanism, and biochemistry*, Springer Science & Business Media, 2005; (*b*) I. Schuster, *Cytochrome P-450: biochemistry and biophysics*, Hemisphere Pub, 1989; (*c*) R. H. Holm, *Chem. Rev.*, 1987, **87**, 1401–1449; (*d*) R. H. Holm, *Coord. Chem. Rev.*, 1990, **100**, 183–221.

11 (*a*) L. I. Hochstein and G. A. Tomlinson, *Annu. Rev. Microbiol.*, 1988, **42**, 231–261; (*b*) W. H. Campbell, *Annu. Rev. Plant Physiol. Plant Mol. Biol.*, 1999, **50**, 277–303.

12 (*a*) K. D. Karlin, *Science*, 1993, **261**, 701–708; (*b*) C. Perez-Rizquez, A. Rodriguez-Otero and J. M. Palomo, *Org. Biomol. Chem.*, 2019, **17**, 7114–7123.

13 (*a*) G. B. Richter-Addo, P. Legzdins and J. Burstyn, *Chem. Rev.*, 2002, **102**, 857–860; (*b*) C. Bogdan, *Nat. Immunol.*, 2001, **2**, 907–916; (*c*) L. Jia, C. Bonaventura, J. Bonaventura and J. S. Stamler, *Nature*, 1996, **380**, 221–226; (*d*) R. F. Furchgott, *Angew. Chem., Int. Ed.*, 1999, **38**, 1870–1880; (*e*) L. J. Ignarro, *Biosci. Rep.*, 1999, **19**, 51–71; (*f*) L. J. Ignarro, *Nitric Oxide: Biology and Pathobiology*, Academic press, 2000.

14 B. Voetsch, R. C. Jin and J. Loscalzo, *Histochem. Cell Biol.*, 2004, **122**, 353–367.

15 C. S. Wilcox, *Am. J. Physiol.: Regul., Integr. Comp. Physiol.*, 2005, **289**, R913–R935.

16 C. Baylis, *Am. J. Physiol. Ren. Physiol.*, 2008, **294**, F1–F9.

17 (*a*) F. Vargas, J. M. Moreno, R. Wangensteen, I. Rodriguez-Gomez and J. Garcia-Estan, *Eur. J. Endocrinol.*, 2007, **156**, 1–12; (*b*) S. Cook, O. Hugli, M. Egli, P. Vollenweider, R. Burcelin, P. Nicod, B. Thorens and U. Scherrer, *Swiss Med. Wkly.*, 2003, **133**, 360–363.

18 (*a*) L. Castillo, T. C. deRojas, T. E. Chapman, J. Vogt, J. F. Burke, S. R. Tannenbaum and V. R. Young, *Proc. Natl. Acad. Sci. U. S. A.*, 1993, **90**, 193–197; (*b*) R. M. Palmer, D. S. Ashton and S. Moncada, *Nature*, 1988, **333**, 664–666.

19 B. A. Averill, *Chem. Rev.*, 1996, **96**, 2951–2964.

20 (*a*) Q. Liu and S. S. Gross, *Methods Enzymol.*, 1996, **268**, 311–324; (*b*) C. Nathan and Q. W. Xie, *J. Biol. Chem.*, 1994, **269**, 13725–13728.

21 (*a*) B. A. Averill, *Chem. Rev.*, 1996, **96**, 2951–2964; (*b*) J. O. Lundberg, E. Weitzberg and M. T. Gladwin, *Nat. Rev. Drug Discovery*, 2008, **7**, 156–167.

22 (*a*) R. Radi, *Proc. Natl. Acad. Sci. U. S. A.*, 2004, **101**, 4003–4008; (*b*) C. H. Lim, P. C. Dedon and W. M. Deen, *Chem. Res. Toxicol.*, 2008, **21**, 2134–2147.

23 (*a*) G. B. Richter-Addo and P. Legzdins, *Metal nitrosyls*, Oxford University Press, 1992; (*b*) P. C. Ford and I. M. Lorkovic, *Chem. Rev.*, 2002, **102**, 993–1018; (*c*) G. R. Wyllie and W. R. Scheidt, *Chem. Rev.*, 2002, **102**, 1067–1090; (*d*) N. Lehnert, E. Kim, H. T. Dong, J. B. Harland, A. P. Hunt, E. C. Manickas, K. M. Oakley, J. Pham, G. C. Reed and V. S. Alfaro, *Chem. Rev.*, 2021, **121**(24), 14682–14905.

24 (*a*) S. Das, Kulbir, S. Ghosh, S. Chandra Sahoo and P. Kumar, *Chem. Sci.*, 2020, **11**, 5037–5042; (*b*) B. Mondal, D. Borah, R. Mazumdar and B. Mondal, *Inorg. Chem.*, 2019, **58**, 14701–14707; (*c*) S. Ghosh, H. Deka, Y. B. Dangat, S. Saha, K. Gogoi, K. Vanka and B. Mondal, *Dalton Trans.*, 2016, **45**, 10200–10208.

25 (*a*) G. Metzker, P. P. Lopes, A. C. da Silva, S. C. da Silva and D. W. Franco, *Inorg. Chem.*, 2014, **53**, 4475–4481; (*b*) A. Sacco, G. Vasapollo and P. Giannoccaro, *Inorg. Chim. Acta*, 1979, **32**, 171–174; (*c*) C. B. Ungermann and K. G. Caulton, *J. Am. Chem. Soc.*, 1976, **98**, 3862–3868; (*d*) K. J. Franz and S. J. Lippard, *Inorg. Chem.*, 2000, **39**, 3722–3723; (*e*) J. Armor, *Inorg. Chem.*, 1973, **12**, 1959–1961; (*f*) P. Kumar, Y. M. Lee, L. Hu, J. Chen, Y. J. Park, J. Yao, H. Chen, K. D. Karlin and W. Nam, *J. Am. Chem. Soc.*, 2016, **138**, 7753–7762.

26 R. L. Roberts, D. W. Carlyle and G. L. Blackmer, *Inorg. Chem.*, 2002, **14**, 2739–2744.

27 X. H. Mu and K. M. Kadish, *Inorg. Chem.*, 1990, **29**, 1031–1036.

28 M. P. Doyle, R. A. Pickering, R. L. Dykstra and B. R. Cook, *J. Am. Chem. Soc.*, 1982, **104**, 3392–3397.

29 P. Kumar, Y. M. Lee, L. Hu, J. Chen, Y. J. Park, J. Yao, H. Chen, K. D. Karlin and W. Nam, *J. Am. Chem. Soc.*, 2016, **138**, 7753–7762.

30 Kulbir, S. Das, T. Devi, M. Goswami, M. Yenuganti, P. Bhardwaj, S. Ghosh, S. C. Sahoo and P. Kumar, *Chem. Sci.*, 2021, **12**, 10605–10612.

31 (*a*) H. Lewandowska, in *Nitrosyl Complexes in Inorganic Chemistry, Biochemistry and Medicine I*, ed. D. M. P. Mingos, Springer Berlin Heidelberg, Berlin, Heidelberg, 2014, DOI: 10.1007/430_2013_109, pp. 115–165; (*b*) A. Yokoyama, J. E. Han, J. Cho, M. Kubo, T. Ogura, M. A. Siegler, K. D. Karlin and W. Nam, *J. Am. Chem. Soc.*, 2012, **134**, 15269–15272.

32 (*a*) J. H. Enemark and R. D. Feltham, *Coord. Chem. Rev.*, 1974, **13**, 339–406; (*b*) A. P. Hunt and N. Lehnert, *Acc. Chem. Res.*, 2015, **48**, 2117–2125.

33 D. J. Thomas and N. Lehnert, in *Reference Module in Chemistry, Molecular Sciences and Chemical Engineering*, Elsevier, 2017, DOI: 10.1016/b978-0-12-409547-2.11678-6.

34 (*a*) J. R. Norton, J. P. Collman, G. Dolcetti and W. T. Robinson, *Inorg. Chem.*, 1972, **11**, 382–388; (*b*) J. L. Brumaghim, J. G. Priepot and G. S. Girolami, *Organometallics*, 1999, **18**, 2139–2144; (*c*) K. A. Kubat-Martin, M. E. Barr, B. Spencer and L. F. Dahl, *Organometallics*, 1987, **6**, 2570–2579; (*d*) R. M. Kirchner, T. J. Marks, J. S. Kristoff and J. A. Ibers, *J. Am. Chem. Soc.*, 1973, **95**, 6602–6613.

35 (*a*) R. Mas-Balleste, A. R. McDonald, D. Reed, D. Usharani, P. Schyman, P. Milko, S. Shaik and L. Que Jr, *Chem.–Eur. J.*, 2012, **18**, 11747–11760; (*b*) S. K. Sharma, A. W. Schaefer, H. Lim, H. Matsumura, P. Moënne-Loccoz, B. Hedman, K. O. Hodgson, E. I. Solomon and K. D. Karlin, *J. Am. Chem. Soc.*, 2017, **139**, 17421–17430.

36 J. A. McCleverty, *Chem. Rev.*, 1979, **79**, 53–76.

37 G. L. Miessler, P. J. Fischer and D. A. Tarr, *Inorganic Chemistry*, Pearson, fifth edn, 2014, pp. 439–441.

38 M. Yenuganti, S. Das, Kulbir, S. Ghosh, P. Bhardwaj, S. S. Pawar, S. C. Sahoo and P. Kumar, *Inorg. Chem. Front.*, 2020, **7**, 4872–4882.